Electronic Supplementary Material (ESI) for Chemical Communications

Tunability by alkali metal cations of photoinduced charge separation in azacrown functionalized graphene

Rafael Ballesteros,[a] Maykel de Miguel,[a] Antonio Doménech-Carbó,[b] Mercedes Alvaro,[a] Hermenegildo Garcia[a,*]

Supporting information

S1. Experimental details

All reagent were purchased from commercially firms and were employed without extra purification. Raman spectra were recorded at ambient temperature with a 514 nm laser excitation on a *Renishaw In Via* Raman spectrometer equipped with a CCD detector. TEM images were recorded in a Philips CM300 FEG system with an operating voltage of 100 kV. XPS spectra were recorded on a SPECS spectrometer equipped with a Phoibos 150 9MCD detector using a non-monochromatic X-ray source (Al and Mg) operating at 200 W. The samples were evacuated in the prechamber of the spectrometer at 1 x 10-9 mbar. Electrochemical experiments have been performed at films of L@GO mechanically deposited on paraffin-impregnated graphite electrodes (PIGEs) following reported procedures [1,2]. The resulting modified electrodes were immersed into well deaerated 0.10 M CsCl, KCl, NaCl and LiCl (Merck reagents) aqueous solutions. Experiments in dry MeCN (Carlo Erba) were performed using Bu_4NPF_6 and $LiClO_4$ (Fluka reagents) in concentration 0.10 M as supporting electrolytes. Ferrocene (Fluka) was used as a complementary electroactive probe in such experiments. Measurements were carried out in a cell thermostated at 298±1 K using a CH 660I potentiostat. A conventional three-electrode arrangement was used with a AgCl (3M NaCl)/Ag reference electrode separated from the bulk solution by a salt bridge and a platinum mesh auxiliary electrode. Cyclic voltammetry (CV) and square wave voltammetry (SWV) were used as detection modes.

S2. Preparation of 1

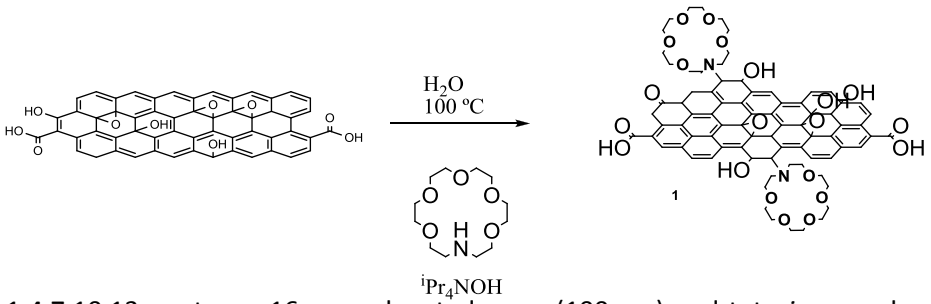

At 25 ºC the 1,4,7,10,13-pentaoxa-16-azacyclooctadecane (100 mg) and tetra*iso*propyl ammonium hydroxide (1M in water, 5 mL) were added to an aqueous solution of GO (0.5 mg/mL) (100 mg, 200 mL). The mixture was stirred and heated up slowly to 100 ºC. The temperature was maintained during 12 hours, and the allowed to reach 25ºC. The reaction mixture was filtrated over a Nylon membrane (0.2 μm pore diameter) and washed with milliq water. The corresponding solid was suspended in water by means of ultrasonication and filtrated again. This procedure was repeated 4 more times. Then the remaining materials was suspended in the small quantity of water (100 mL) with ultrasonication and lyophilized to afford 1 as a black powder (95 mg). The corresponding combustion analysis afforded: H 1.216% C 45.688% N 2.532% S 0.000%.

S3. Characterization of 1

S3.1 ^{13}C-NMR

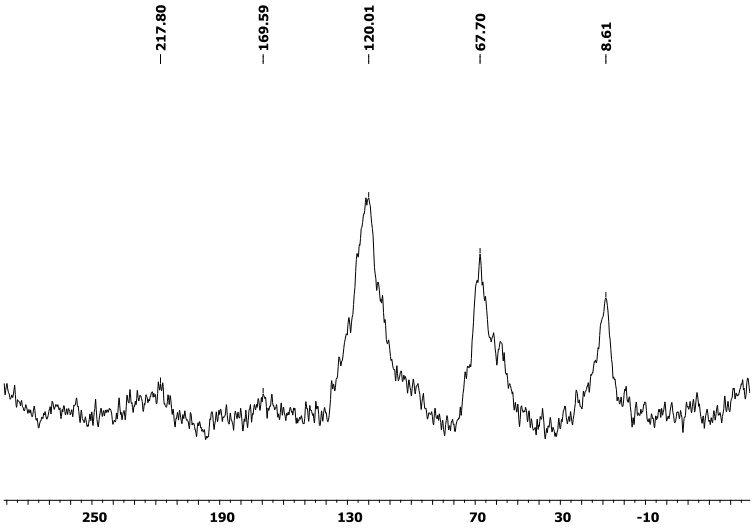

S3.2 ^{1}H-NMR

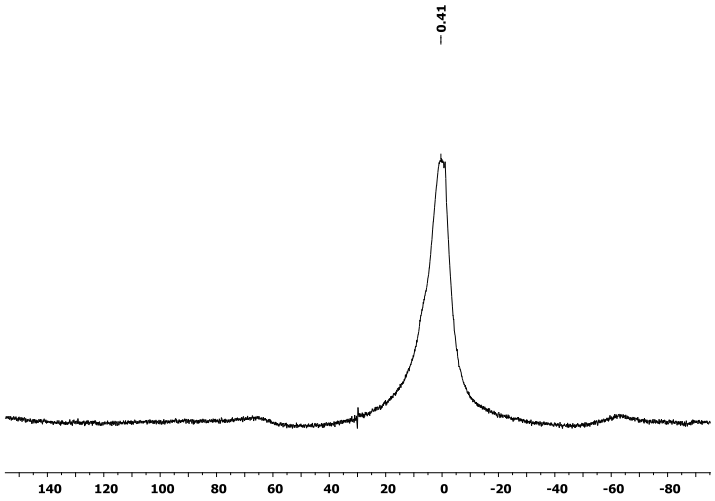

S3.3 HETCOR ^{13}C-^{1}H spectra of 1.

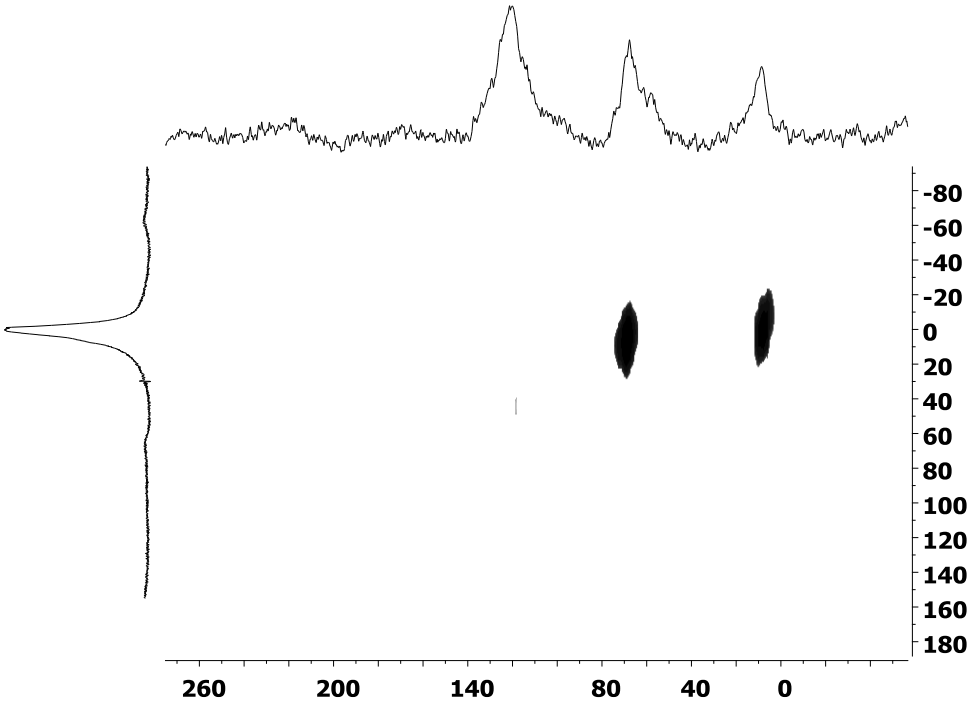

S3.4 G in Nitrogen atmosphere: 1

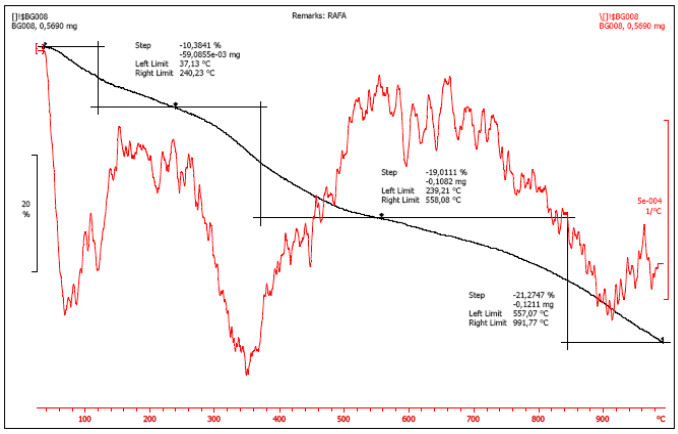

Starting GO

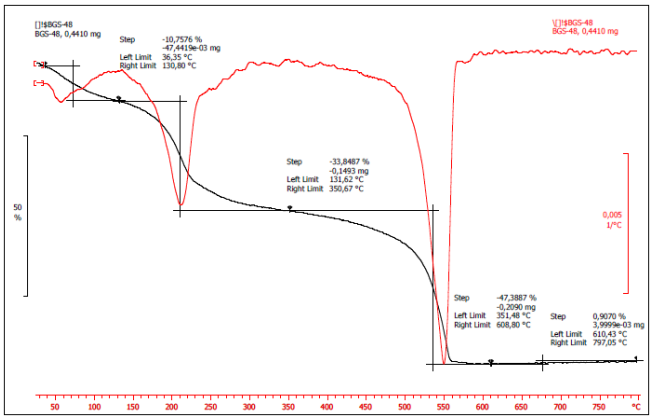

S3.5 FT- IR spectra

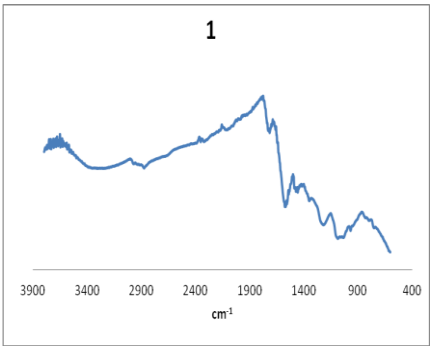

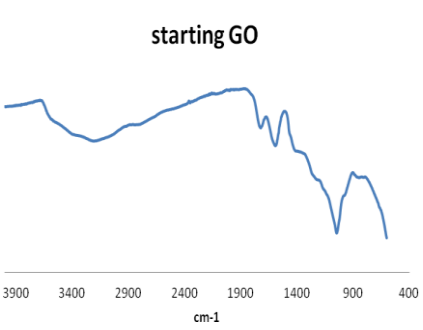

S3.6 RAMAN:

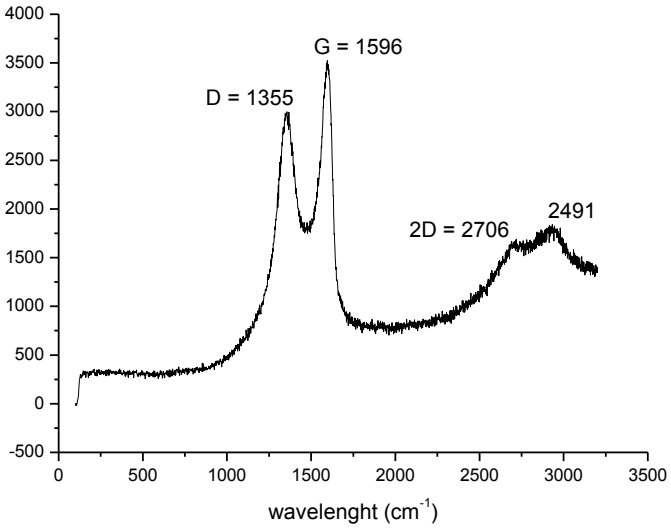

S3.7 XPS:

Group	Name	Position	FWHM	Line Shape	R.S.F.	Area	% Conc.
	O1s 2	533.44	3.275	GL(30)	1	27115.6	48.22
C-O, C-N	**C1s 3**	286.92	2.807	GL(30)	1	19908.7	35.404
C=C	**C1s 3**	285.56	1.362	GL(30)	1	5812.3	10.336
C=O, COO	**C1s 3**	289.98	2.52	GL(30)	1	2052.7	3.65
Amine	**N1s**	394.92	2.02	GL(30)	1.8	418.5	0.413
NH+	**N1s**	401.19	5.155	GL(30)	1.8	1823.2	1.801
Imine	**N1s**	396.75	1.844	GL(30)	1.8	177.5	0.175

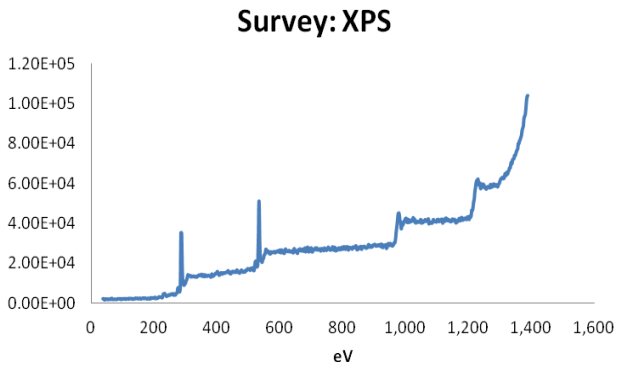

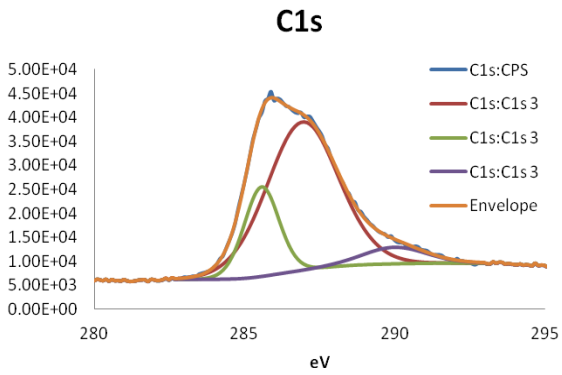

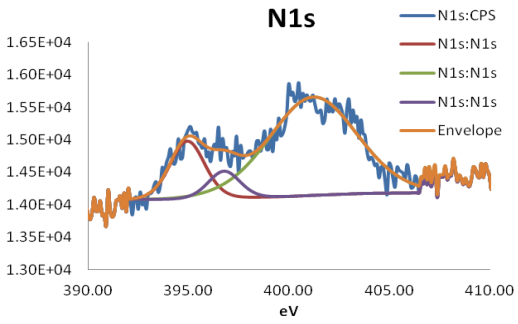

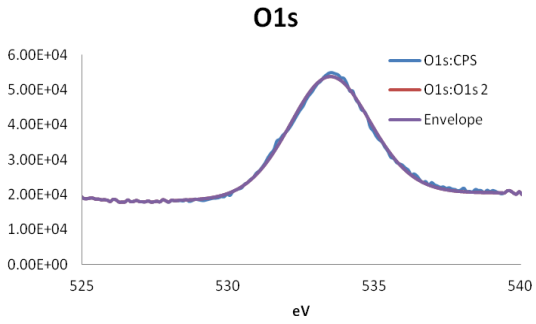

S3.8 Selected TEM images:

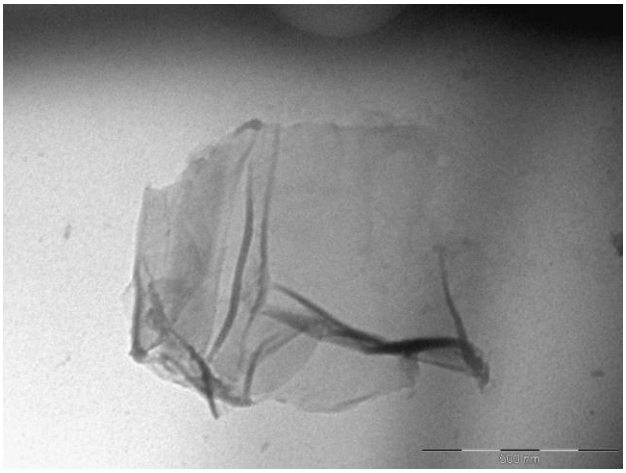

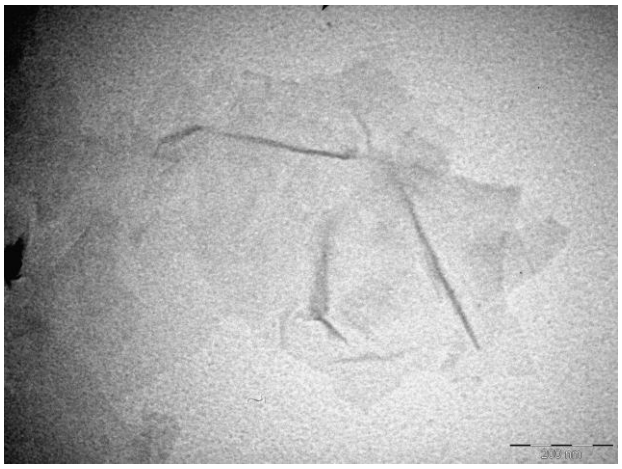

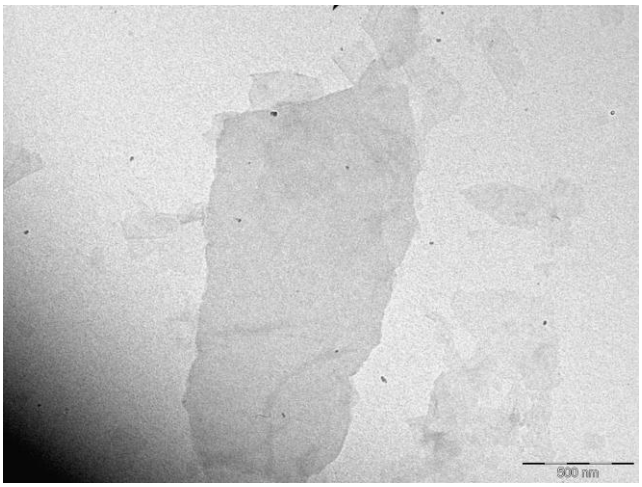

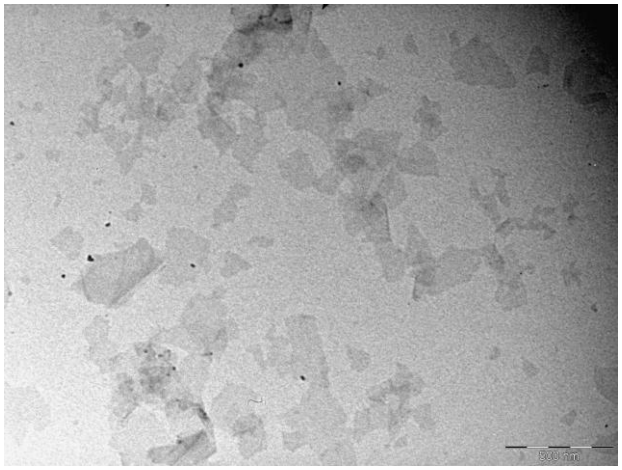

Preparation of Na-1 And ^{13}C-NMR .

At 25 º C $NaBF_4$ (100 mg, excess) was added to a solution of **1** (100 mg in 200 mL of milli q water) the mixture was stirred during 5 hours and then filtrated over a Nylon membrane ((0.2 μm pore diameter) and washed with milliq water. This protocol was repeated 3 more times. Then the crude was solved in milli q water and liofilized.

Comparation of 13C-NMR Spectra of **1** (up) and **Na-1** (dowm)

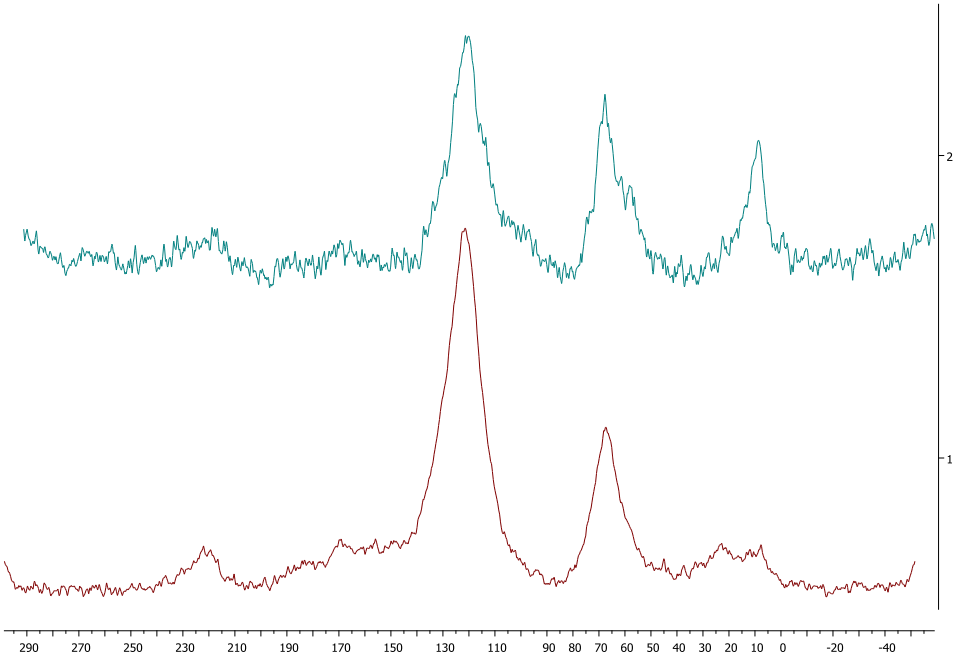

S5 Electrochemical studies

Results and discussion

Fig. S5.1a compares CVs for L@GO-modified PIGEs immersed into 0.10 M CsCl and 0.10 M NaCl aqueous solutions. The voltammograms exhibit a cathodic wave ca. -0.65 V vs. couples with a weaker anodic signal at ca. -0.20 V. These voltammetric features are close to those reported in literature for the reduction of graphene oxide (GO) in contact with a conducting base electrode in neutral or weakly alkaline - and Na^+ (or Li^+) containing aqueous media [3-5]. The peak currents and the gross typical capacitive background current are larger in NaCl (as well as in LiCl and KCl) than in CsCl, in turn being larger than that recorded at the unmodified PIGE. To rationalize these features, it should be noted that, as far as GO is an insulating material, its electrochemical reduction involves doping with electrolyte cations. This process removes oxygen from GO producing RGO at the graphene/base electrode/electrolyte three-phase boundary while electrolyte cations are intercalated between GO layers [6,7]. In our case, functional aza-ether crown groups must produce a size-selectivity effect, allowing for the incorporation of Li^+, Na^+ and K^+ cations, but blocking the entrance of bulky Cs^+ ones. It should be emphasized, however, that the process used to reduce/oxidize GO changes simultaneously the amounts of edge-plane-like sites and defects in GO and GRO. As far as such sites exhibit high electrochemical activity, the effects due to such sites are superimposed to those due to functional groups [8,9]. As a result, although the voltammetric currents for GO reduction are clearly lower in contact with CsCl electrolyte than in contact with LiCl, NaCl and KCl solutions, they become lightly enhanced relative to unmodified electrodes. Consistently, subtraction of CV in =.10 M CsCl from the CV in 0.10 M NaCl **(Fig. S5.1b**), shows clearly the voltammetric features corresponding to the reduction of GO to RGO at -0.65 V and the subsequent oxidation of the later at -0.2 V.

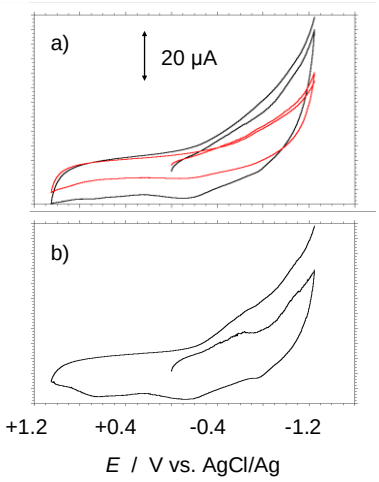

Figure S5.1. a) CVs for L@GO-modified PIGEs immersed into 0.10 M CsCl (red line) and 0.10 M NaCl (black line) aqueous solutions; b) subtracted voltammetric curve obtained from the above CVs . Potential scan rate 50 mV/s.

In order to re-assess size-selective effects in L@GO, a second series of experiments was performed in MeCN comparing the voltammetry of this material immersed into electrolytes containing size-allowed Li^+ and bulky, size-hindered Bu_4N^+ ions. **Figure S5.2** shows SWVs for L@GO-modified PIGEs immersed into 0.10 M Bu_4NPF_6/MeCN and 0.10 M Bu_4NPF_6 plus 0.02 M $LiClO_4$/MeCN and 0.10 M $LiClO_4$/MeCN. Again, the cathodic wave between -0.80 and -1.20 V is considerably enhanced in the presence of Li^+ ions and increases as the concentration of such ions increases.

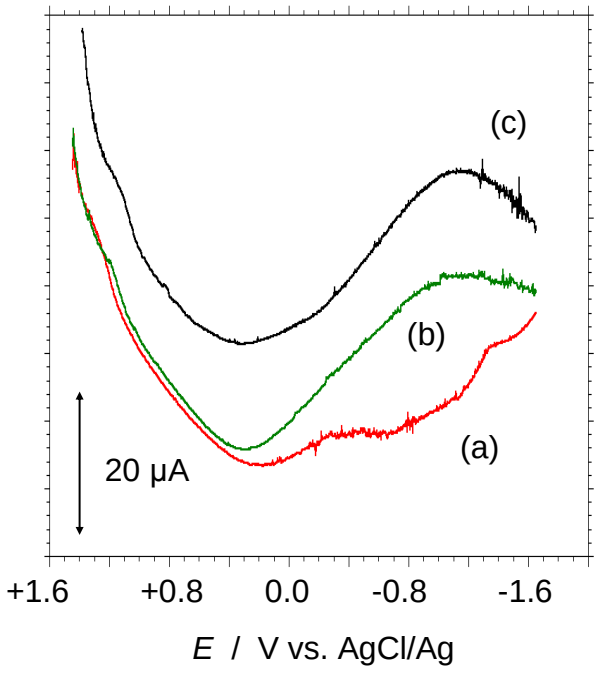

Figure S5.2. SWVs for L@GO-modified PIGEs immersed into: a) 0.10 M Bu_4NPF_6/MeCN; b) 0.10 M Bu_4NPF_6/MeCNplus 0.02 M $LiClO_4$/MeCN; c) 0.10 M Bu_4NPF_6/MeCNplus 0.10 M $LiClO_4$/MeCN. Potential scan initiated at +1.25 V in the negative direction; potential step increment 4 mV; square wave amplitude 25 mV; frequency 5 Hz.

To corroborate the reductive nature of such signal, voltammograms in air-saturated, ferrocene-containing solutions were carried out. The corresponding results are shown in **Fig. S5.3**. Here, the reduction of dissolved oxygen at ca. -1.0 V, a well-known electrochemical process in nonaqueous media [10-13], is accompanied by the well-defined reversible couple for ferrocene oxidation at +0.50 V. As expected, the oxygen reduction peak is clearly enhanced at L@GO-modified electrodes in contact with Li^+-containing electrolytes relative to those

containing Bu_4N^+. This feature agrees with the recognized catalytic ability exerted by graphenes on electrochemical O_2 reduction [9,14].

The most remarkable effect, however, can be seen on comparing the peak current in the first and second scan when the potential is switched beyond the GO reduction signal, for ferrocene oxidation in CVs initiated at 0.0 V in the negative (**Fig. S5.3a**) and positive directions (**Fig. S5.3a**). In Bu_4N^+-containing electrolytes, the peak current for ferrocene oxidation is essentially identical in the first and second scans regardless the direction of the initial scan, as expected for L@GO which is not electrochemically modified during electrochemical turnovers. In contrast, in Li^+-containing electrolytes, the peak current for ferrocene oxidation is clearly enhanced in anodic scans initiated at potentials more negative than -0.80 V; i.e., those corresponding to the reduction of GO relative to those initiated at potentials less negative than -0.80 V. This can be clearly seen in Fig. 3b, where the peak current for the second scan, initiated at -1.25 V, is significantly enhanced with respect to those in the first scan, initiated at 0.0 V. This suggests that, in the presence of Li^+, L@GO is effectively reduced, resulting in an electrocatalytically active form.

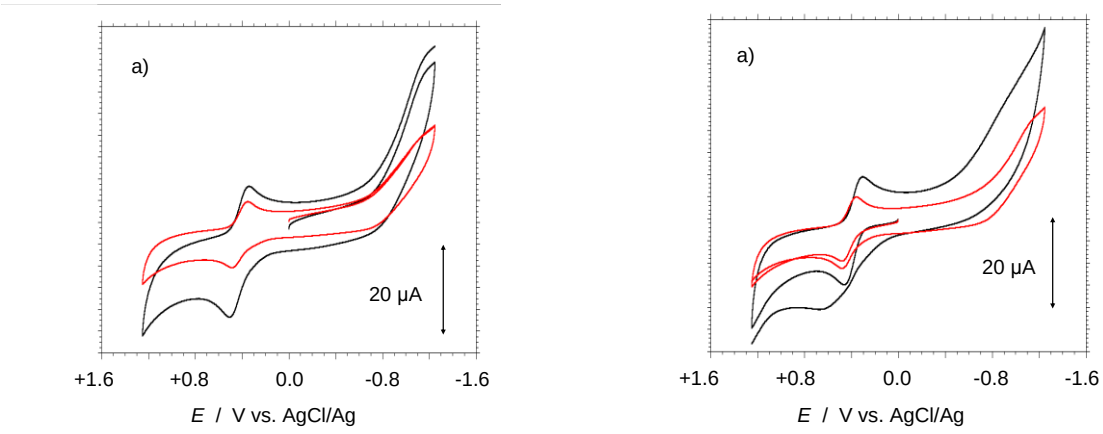

Figure S5.3. CVs for L@GO-modified PIGEs immersed into air-saturated 1.0 mM ferrocene solutions using as supporting electrolytes 0.10 M Bu_4NPF_6/MeCN (red lines) and 0.10 M Bu_4NPF_6 plus 0.01 M $LiClO_4$/MeCN (black lines). Potential scan initiated at 0.0 V: a) in the negative; b) in the positive direction. Potential scan rate 250 mV/s.

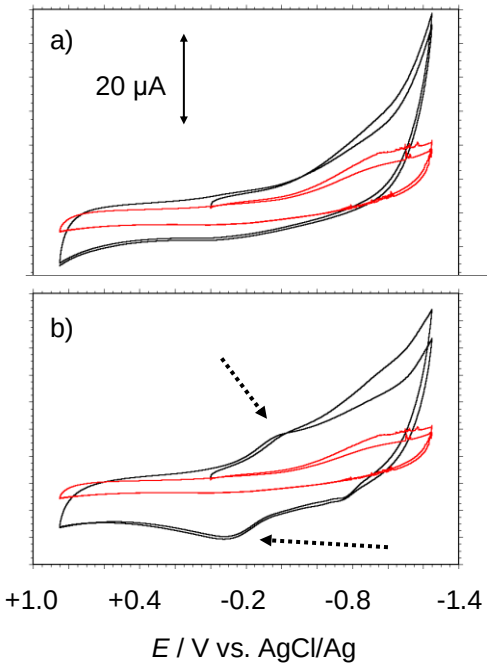

Figure S5.4. Comparison of cyclic voltammograms at: a) **1**-modified, b) GO-modified graphite electros (blanck lines) and unmodified graphite electrode (red lines) immersed into an aqueous 0.10 M $LiClO_4$ solution. Potencial scan rate 100 mV/s. Arrows indicate peaked responses appearing at electrodes modified with functionalized GO.

The $Fe(CN)_6^{4-}$ is used here as a redox probe (such as ferrocene in Figure S5.3) displaying an essentially reversible oxidation at ca. +0.15 V. In voltammograms initiated at 0.0 V in the positive direction, the oxidation peak for hexacyanoferrate(II) oxidation recorded in the initial anodic scan is mainly due, under our experimental conditions (microparticulate graphene film on an inert base electrode), to the hexacyanoferrate ions reaching the base electrode and grapheme surfaces. As far as the grapheme increases the conductivity and effective surface area, the voltammetric signals are in general enhanced at graphene-modified electrodes relative to the base electrode alone with no influence of the electrolyte cation. However, if the potential is switched at values negative enough to promote the reduction of GO to reduced GO (RGO), the intensity of the peak for hexacyanoferrate(II) oxidation which appears in the second scan, depends on the electrolyte cation. This effect can be attributed to the moderate catalytic effect exerted by reduced graphene oxide (GOR) on hexacyanoferrate(II) oxidation. During the cathodic scan preceding the second anodic scan, functionalized GO is reduced to GOR by means of a cation-mediated process. Then, the peak current for hexacyanoferrate oxidation is larger in the second scan relative to the first scan (where no GO reduction to RGO occurred) in voltammograms for Li^+ and weakly for Na^+ and K^+ salts while no peak current enhancement occurred for Cs^+.

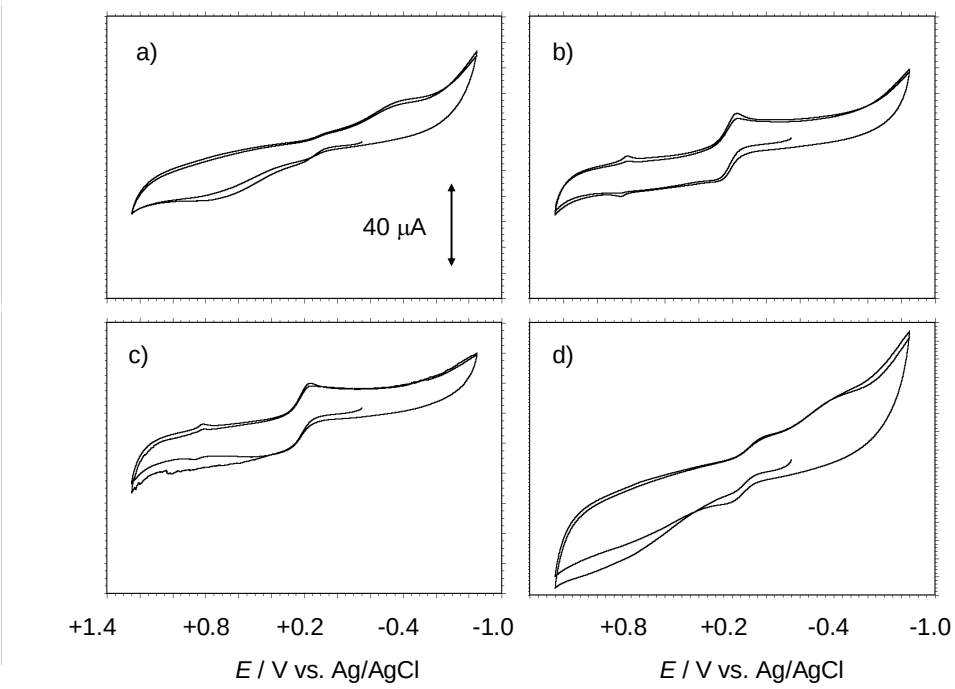

Figure S.5.5. Cyclic voltammograms at **1**-modified electrodes immersed into 5.0 mM $K_4Fe(CN)_6$ solutions in: a) 0.10 M CsCl; b) 0.10 M KCl; c) 0.10 M NaCl; d) 0.10 M LiCl. Potential scan rate 50 mV/s.

Figures S.5.5 and S.5.6 complement the above observations using square wave voltammetry. For Cs^+, the peak current for hexacyanoferrate(II) oxidation is essentially the same regardless the starting potential. In contrast, for Li+, the peak current for that process increases if the potential is scanned from values negative enough to promote the cation-assisted reduction of GO. Interestingly, in the presence of Li^+, the voltammogram exhibits

peak splitting, suggesting that effective Li^+-assisted GO reduction results in the formation of additional catalytic sites for hexacyanoferrate oxidation.

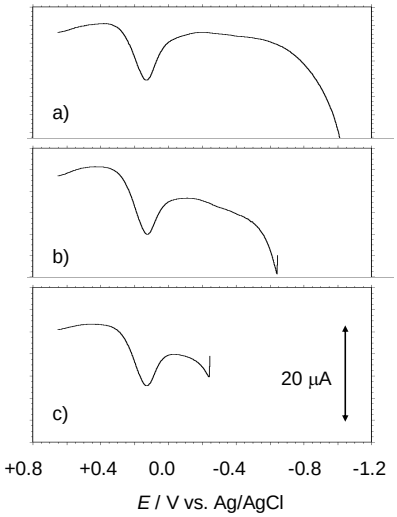

Figure S.5.6 Square wave voltammograms at **1**-modified electrodes immersed into 5.0 mM $K_4Fe(CN)_6$ solution in 0.10 M CsCl. Potential scan initiated at: a) -1.05; b) -0.65; c) -0.25 V in the positive direction. Potential step increment 4 mV; square wave amplitude 25 mV; frequency 10 Hz.

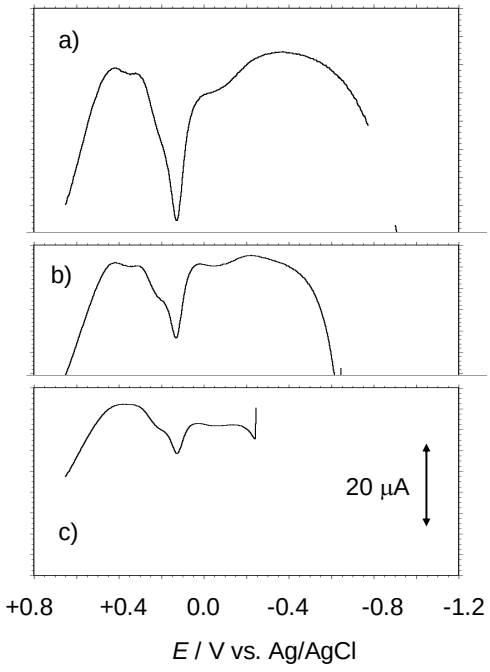

Figure S.5.7. Square wave voltammograms at **1**-modified electrodes immersed into 5.0 mM $K_4Fe(CN)_6$ solution in 0.10 M LiCl. Potential scan initiated at: a) -1.05; b) -0.65; c) -0.25 V in the positive direction. Potential step increment 4 mV; square wave amplitude 25 mV; frequency 10 Hz.

S6 Laser Flash Photolysis

Molar concentrations of the corresponding wáter solutions of (M) BF4
Na = 0.039 M; K =0.029 M y Li= 0.06 M y Cs = 0.06 M

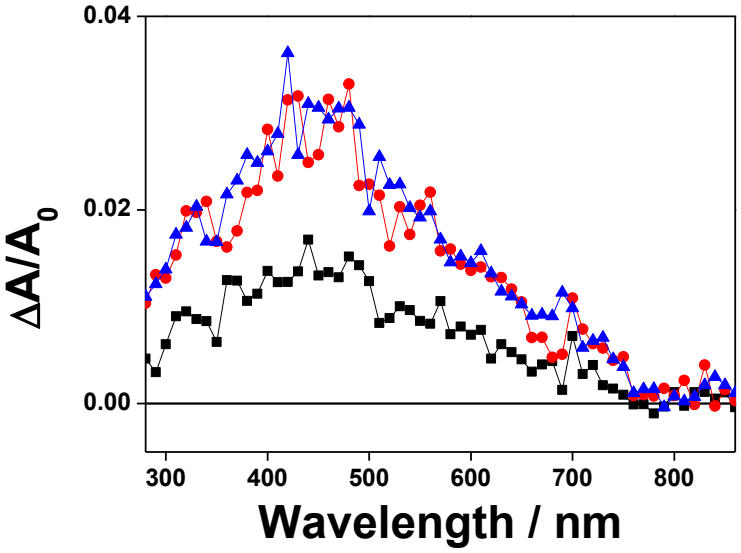

Figure S6.1.- Transient spectra of a N_2 purged graphene with azacrown solution (0.025 mg/mL) in water recorded at 25 μs after 355 nm laser flash upon addition of increasing amount of k^+: 0 (■), X(●) and X(▲) mg/L

	t1(μs)	t2(μs)
Inicial	33.25	579
10 μL	22.45	572
15 μL	40.53	778

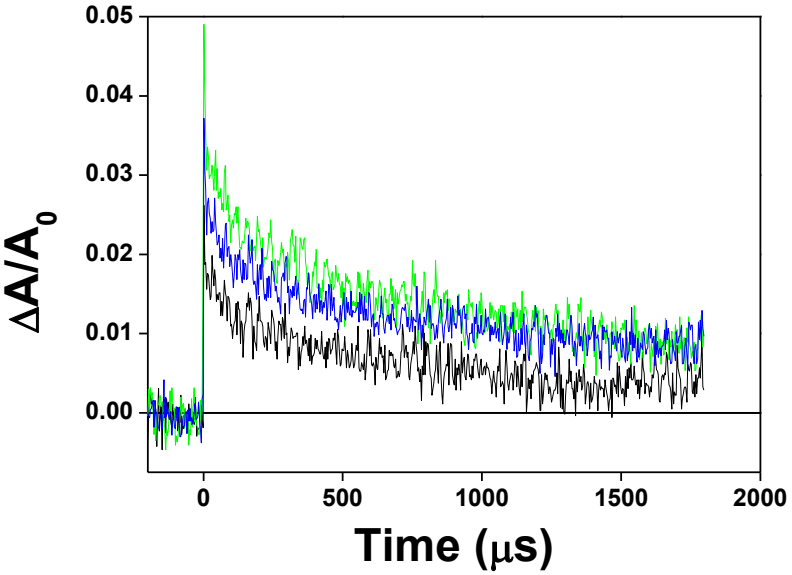

Figure S6.2: Signal decays (plotted as the relative variation of the signals, A) monitored at 460 nm recorded for graphene with azacrown after 355 nm laser flash containing 0 (black), 10 (blue), and 15 (green) μL K^+.
Na

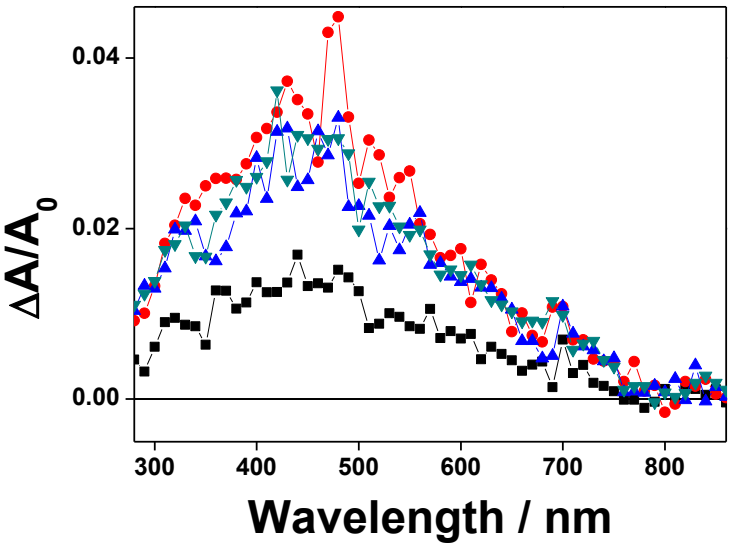

Figure S6.3.- Transient spectra of a N_2 purged graphene with azacrown solution (0.025 mg/mL) in water recorded at 25 μs after 355 nm laser flash upon addition of increasing amount of Na^+: 0 (■), 5 (●) and 15(▲)μL (mg/L)

	t1(μs)	t2(μs)
Inicial	**33.25**	**579**
10 μL	**62.61**	**773**
15 μL	**73.37**	**1316**

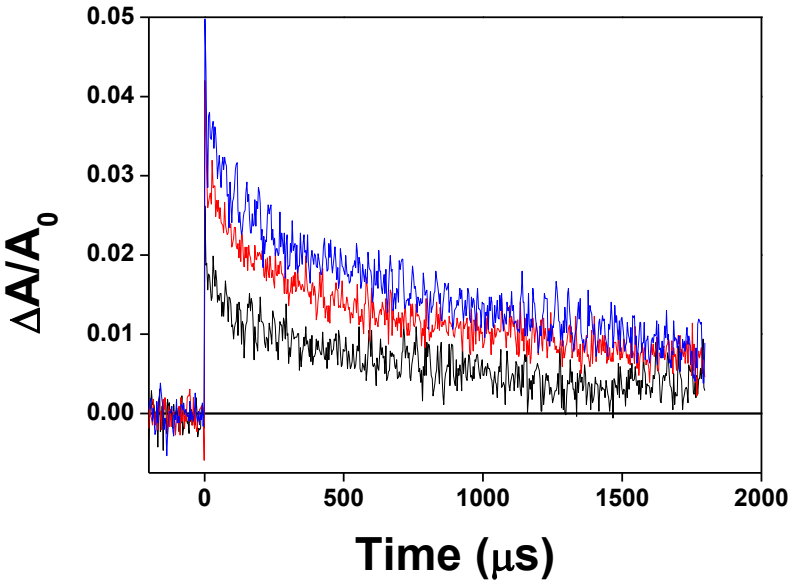

Figure S6.4: Signal decays (plotted as the relative variation of the signals, A) monitored at 460 nm recorded for graphene with azacrown after 355 nm laser flash containing 0 (black), 5 (red), and 15 (blue) μL (mg L^{-1}) Na^{+}.

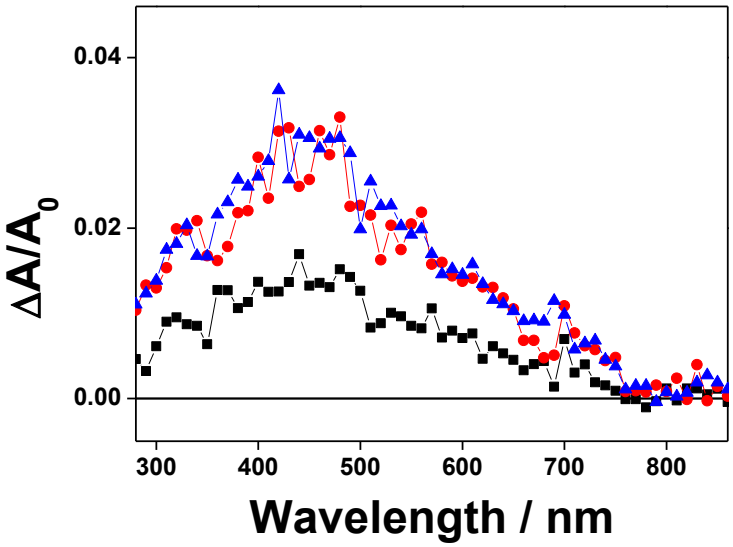

Li

Figure S6.5.- Transient spectra of a N_2 purged graphene with azacrown solution (0.025 mg/mL) in water recorded at 25 μs after 355 nm laser flash upon addition of increasing amount of Li^{+}: 0 (■), 5 (●) and 10(▲) μL

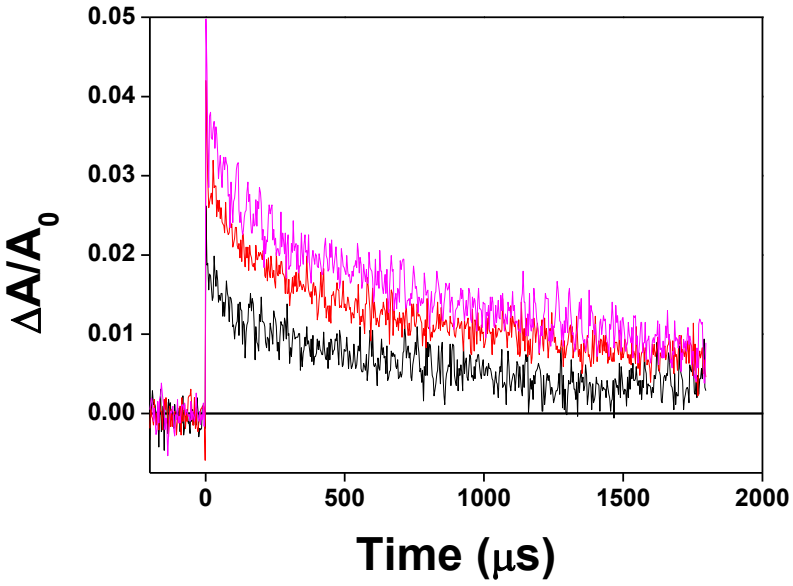

Figure S6.6: Signal decays (plotted as the relative variation of the signals, A) monitored at 460 nm recorded for graphene with ether crown after 355 nm laser flash containing 0 (black), 0.08 (blue), and 5 (green) mg L^{-1} Li^{+}.

	t1(μs)	t2(μs)
Inicial	**34.55**	**569**
5 μL	**62.53**	**767**
10 μL	**74.55**	**1247**

Cs

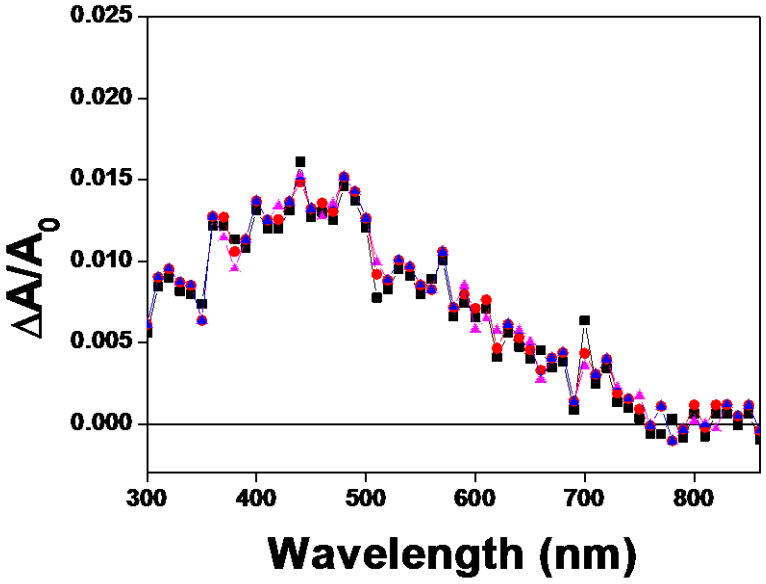

Figure S6.7.- Transient spectra of a N_2 purged graphene with ether crown solution (0.025 mg/mL) in water recorded at 25 μs after 355 nm laser flash upon addition of increasing amount of Cs^{+}: 0 (■), 0.08 (●) and 5(▲) mg/L

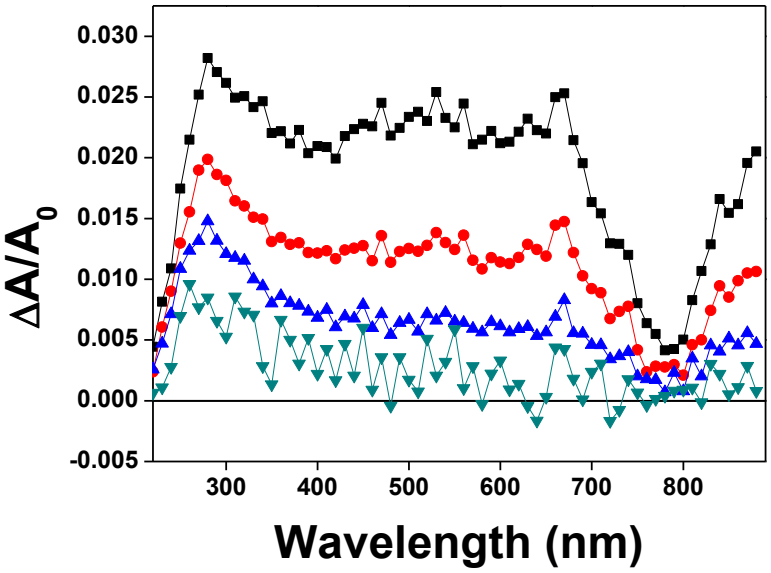

Figure S6.8.- Transient spectra of a N_2O purged graphene with azacrown solution (0.025 mg/mL) in water recorded at 51 (■),160 (●) 448(▲) and 2793 μs after 355 nm laser flash.

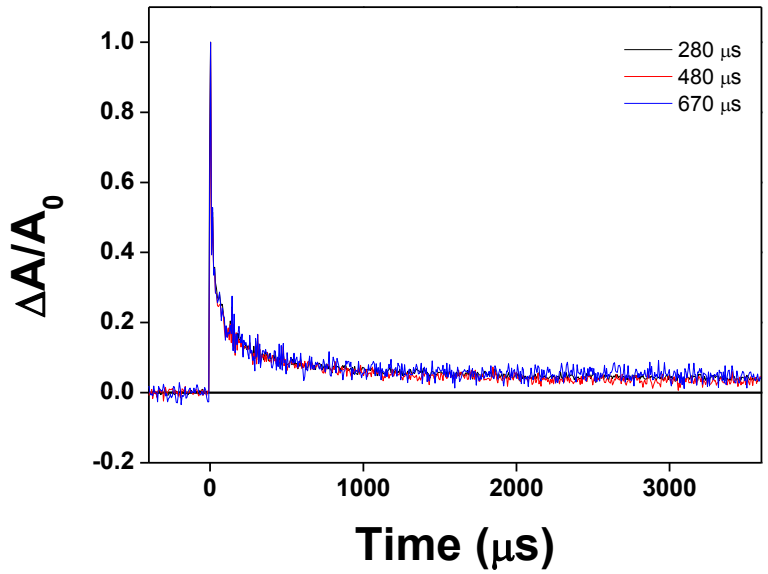

Figure S6.9: Signal decays (plotted as the relative variation of the signals, A) of graphene purged with N_2O monitored at 280 nm (black), 480 nm (red line) and 67y0 nm (blue line) after 355 nm laser flash.

S7. References

1. Scholz, F.; Meyer, B. *Electroanalytical Chemistry, A Series of Advances* (Bard, A.J.; Rubinstein, I. Eds.), Marcel Dekker, New York, 1998, 20, 1-86.

2. Scholz, F.; Schröder, U.; Gulaboski, R. *Electrochemistry of Immobilized Particles and Droplets*, Springer, Berlin, 2005.
3. Kotov, N.A.; Dekany, I.; Fendler, J.H. *Adv. Mater*. 1996, 8, 637-641.
4. M. Zhou, Y. Wang, Y. Zhai, J. Zhai, W. Ren, F. Wang and S. Dong, *Chem.–Eur. J*., 2009, 15, 6116–6120.
5. Ramesha, G.K.; Sampath, S. *J. Phys. Chem. C* 2009, 113, 7985-7989.
6. Alacantara, R.; Jimenez-Mateos, J.M.; Lavela, P.; Tirado, J.L. *Electrochem. Commun.* 2001, 3,639-642.
7. Shao, Y.; Wang, J.; Engelhard, M.; Wang, C.; Lin, Y. *J. Mater. Chem*. 2010, 20, 743-748.
8. Chen, D.; Tang, L.; Li, J. *Chem. Soc. Rev*. 2010, 39, 3157-3180.
9. Ratinac, K.R.; Yang, W.; Gooding, J.J.; Thordarson, P.; Braet, F. *Electroanalysis* 2011, 23, 803-826.
10. D.T. Sawyer, G. Chiericato, C.T. Angelis, E.J. Nanni, T. Tsuchiya, *Anal. Chem.* **1982**, *54*, 1720-1724.
11. F. Matsumoto, S. Uesugi, M. Harada, N. Koura, T. Ohsaka, *Electrochemistry* **2003**, *71*, 927-932.
12. M.E. Ortiz, L.J. Núñez-Vergara, J.A. Squella, *J. Electroanal. Chem.* **2003**, *549*, 157-160.
13. P.S. Singh, D.H. Evans, *J. Phys. Chem. B* **2006**, *110*, 637-644.
14. Tang, L.H.; Wang, Y.; Li, Y.M.; Feng, H.B.; Lu, J.; Li, J.H. *Adv. Funct. Mater*. 2009, 19, 2782-2789.